Joint Frequency and Timing Recovery for MSK-Type Modulation

Michele Morelli and Umberto Mengali, *Fellow, IEEE*

***Abstract*— We investigate a novel nondata-aided method for jointly estimating timing and carrier frequency offset in MSK-type modulation. The algorithm has a feedforward structure and lends itself to a simple digital implementation. Its estimation accuracy depends on a design parameter that may be varied to trade performance for computational complexity. Setting the parameter to unity yields a synchronization scheme already known in the literature. Computer simulations are used to assess the synchronizer performance on AWGN Rayleigh fading channels with MSK and Gaussian MSK modulation.**

***Index Terms*—Frequency offset, MSK-type modulation, timing offset.**

I. Introduction

CONTINUOUS phase modulation (CPM) is a signaling method with good energy and bandwidth efficiency [1]. Furthermore, it generates constant envelope waveforms and therefore is very attractive with radio channels employing nonlinear power amplifiers. Its main drawback is that a maximum likelihood (ML) detector is generally too complex to implement as it requires a high number of matched filters and a Viterbi processor operating over a large trellis. Fortunately, simpler receiver structures have been devised for the CPM subclass with binary alphabet and modulation index equal to 0.5. These formats are referred to as MSK-type modulations [2] and are adopted in second generation cellular systems like the GSM and the DCS1800.

Knowledge of the symbol timing, carrier phase, and carrier frequency offset is necessary for coherent demodulation of MSK-type signals. Unfortunately, phase estimation is difficult to implement on fading channels and, in fact, differential detection is often resorted to [3]–[6] in these applications. Even with differential detection, however, the problem of symbol timing and frequency offset recovery remains.

Several methods for timing and frequency recovery are based on closed-loop techniques. In [7], the IF signal is passed through a second-order nonlinearity to generate periodic components related to the carrier and clock frequencies. Synchronization is performed by extracting these frequencies by means of phase-locked loops. The risk of false locks is a serious limitation to this method. In [8], a symbol timing loop is proposed in which the samples of the baseband signal are fed to a fourth-order nonlinearity which drives a numerically controlled oscillator. The acquisition time of the loop depends on the initial timing error and may be too long in certain applications. In [9], a data-aided feedforward method for frequency recovery is proposed and applied to Gaussian MSK (GMSK). Although its estimation accuracy is remarkably close to the Cramer–Rao bound, its operating range is limited to a few percents of the bit rate. Reference [10] investigates frequency recovery by means of a delay-and-multiply structure. The acquisition range depends on the delay value and is generally larger than with the method in [9]. However, the estimates are affected by a large amount of self-noise. Joint symbol timing and frequency offset recovery is performed in [11] by means of a nondata-aided (NDA) feedforward structure. This synchronizer is suitable for differential detection receivers and lends itself to a fully digital implementation. Unfortunately, it has been conceived specifically for MSK and its performance with narrow-band modulation (with GMSK, for instance) is poor.

In this paper we propose a symbol timing and frequency offset estimation scheme which is applicable to the entire class of MSK-type signals. Due to its feedforward structure, it is hang-up free and is well-suited for burst-mode transmissions. Its complexity is proportional to an integer parameter M. For $M = 1$ and MSK modulation, the synchronizer coincides with the scheme studied in [11].

The remainder of the paper is organized as follows. The next section provides the signal model and introduces basic notations. In Section III, the novel algorithm is described. Simulation results for AWGN and Rayleigh fading channels are illustrated in Section IV. Finally, some conclusions are drawn in Section V.

II. Signal Model

The complex envelope of an MSK-type signal may be written as

$$s(t) = e^{j\psi(t;\alpha)} \tag{1}$$

where

$$\psi(t;\boldsymbol{\alpha}) = \pi \sum_i \alpha_i q(t - iT) \tag{2}$$

is the information bearing phase. In the above equation, $\boldsymbol{\alpha} = \{\alpha_i\}$ are independent data symbols taking on the values ± 1 with equal probability, T is the symbol period, and $q(t)$ is the

Paper approved by E. Panayirci, the Editor for Synchronization and Equalization of the IEEE Communications Society. Manuscript received April 15, 1998; revised October 8, 1998.

M. Morelli is with the Centro Metodi e Dispositivi Radiotrasmissione, Italian National Research Council, 56126 Pisa, Italy (e-mail: morelli@iet.unipi.it).

U. Mengali is with the Department of Information Engineering, University of Pisa, 56126 Pisa, Italy (e-mail: mengali@iet.unipi.it).

Publisher Item Identifier S 0090-6778(99)05017-5.

phase pulse of the modulator, which is related to the *frequency pulse* $h(t)$ by the relation

$$q(t) = \int_{-\infty}^{t} h(\tau)\, d\tau. \tag{3}$$

The pulse $h(t)$ is time limited to the interval $(0, LT)$ and is normalized so that

$$q(LT) = 1/2. \tag{4}$$

In this study we consider three frequency pulses: rectangular (LREC), raised-cosine (LRC), and Gaussian-MSK (GMSK). Formally

$$\text{LREC: } h(t) = \begin{cases} \dfrac{1}{2LT}, & 0 \le t \le LT \\ 0, & \text{otherwise} \end{cases} \tag{5}$$

$$\text{LRC: } h(t) = \begin{cases} \dfrac{1}{2LT}\left[1 - \cos\left(\dfrac{2\pi t}{LT}\right)\right], & 0 \le t \le LT \\ 0, & \text{otherwise} \end{cases} \tag{6}$$

$$\text{GMSK: } h(t) = \frac{1}{2T}\left\{Q\left[\frac{2\pi B}{\sqrt{\ln 2}}\left(t - \frac{L+1}{2}T\right)\right] - Q\left[\frac{2\pi B}{\sqrt{\ln 2}}\left(t - \frac{L-1}{2}T\right)\right]\right\} \tag{7}$$

where B is a design parameter and $Q(x)$ is defined as

$$Q(x) = \frac{1}{\sqrt{2\pi}} \int_{x}^{\infty} e^{-t^2/2}\, dt. \tag{8}$$

The value of L in (7) is such that $h(t)$ is (practically) limited to the interval $(0, LT)$. In the case $BT = 0.3$ we consider later, this happens for $L \ge 5$. It should be noted that in all of the above cases, the phase pulse satisfies the symmetry condition

$$q(t) = \frac{1}{2} - q(LT - t). \tag{9}$$

For the time being, we assume that $s(t)$ is transmitted over an AWGN channel. Later on, however, the estimator performance will be assessed with either an AWGN channel or with Rayleigh fading. The complex envelope of the received signal is modeled as

$$r(t) = e^{j(2\pi\nu t + \theta)} s(t - \tau) + w(t) \tag{10}$$

where ν and θ represent the frequency offset and the carrier phase, respectively, τ is the timing epoch, and $w(t)$ is a complex-valued white Gaussian noise process. Its real and imaginary parts are independent and have each a two-sided power spectral density $T(E_b/N_0)^{-1}/2$, where E_b represents the received signal energy per symbol.

At the receiver, the incoming waveform is fed to a low-pass filter so as to eliminate out-of-band noise. The filter bandwidth B_w is chosen large enough so as not to distort the signal components even in the presence of (limited) frequency offsets. Thus, letting $x(t)$ be the filter output, we may write

$$x(t) = e^{j(2\pi\nu t + \theta)} s(t - \tau) + n(t) \tag{11}$$

where $n(t)$ is filtered noise. In a digital implementation of the receiver, the waveform $x(t)$ is sampled at some rate $1/T_s$ using a *free-running* oscillator. In this study we choose the sampling rate $1/T_s$ a multiple N of the nominal bit rate and we take the oversampling factor N large enough to avoid aliasing.

Denoting by $x_k(i)$ the sample of $x(t)$ taken at $t = kT + iT_s$, we have

$$x_k(i) = e^{j[\psi(kT + iT_s - \tau; \alpha) + 2\pi\nu(kT + iT_s) + \theta]} + n_k(i) \qquad 0 \le i \le N - 1. \tag{12}$$

In this equation, the index k counts the symbol intervals while i counts the samples within a symbol interval. As the signal component in (12) depends on ν and τ, we may estimate these parameters from the observation of the sample sequence $\{x_k(i)\}$. In doing so, we assume no information about the transmitted symbols (NDA operation). Also, we do not pursue any optimality criterion; our approach is just *ad hoc*. To proceed, we break $\{x_k(i)\}$ into adjoining segments of $N \times L_0$ samples, L_0 being the number of symbols in each segment. Our task is to derive estimates of ν and τ from each subsequence $\{x_k(i)\}_{(l)}$ $(l = 0, 1, \cdots)$. We shall see later how to put the estimates together to form a continuous reference for the receiver. For the moment, we concentrate on the first segment of $\{x_k(i)\}$ and omit the index l throughout.

III. Timing and Frequency Estimation

To begin, consider the m-lag autocorrelation of $x^2(t)$

$$R_m(t) = E\{[x(t)x^*(t - mT)]^2\} \tag{13}$$

where $E\{\cdot\}$ denotes expectation operation. Inserting (11) into (13) yields

$$R_m(t) = e^{j4\pi m\nu T} g_m(t - \tau) + N_m(t) \tag{14}$$

where

$$g_m(t) = E\left\{e^{j2[\psi(t;\alpha) - \psi(t - mT;\alpha)]}\right\} \tag{15}$$

and $N_m(t)$ is a noise term. In the Appendix it is shown that (15) may be put in the form

$$g_m(t) = \prod_{n=-\infty}^{+\infty} \cos[2\pi p_m(t - nT)] \tag{16}$$

where the pulse $p_m(t)$ has support $(0, mT + LT)$ and is related to the phase response of the modulator by the relation

$$p_m(t) = q(t) - q(t - mT). \tag{17}$$

In particular, for MSK modulation (rectangular frequency pulse of length $L = 1$), it can be shown from (3) and (5) that (16) reduces to

$$g_m(t) = \frac{1}{2}(-1)^m \left[1 + \cos\left(\frac{2\pi t}{T}\right)\right]. \tag{18}$$

Returning to (14), it is clear that $R_m(t)$ provides information about the parameters ν and τ. Then, assuming that M autocorrelations are available (say those with indexes from one to M), the question arises of how they can be used to estimate ν and τ. A heuristic procedure is now given in two steps: first we estimate τ independently of ν, and next we exploit this result to estimate ν.

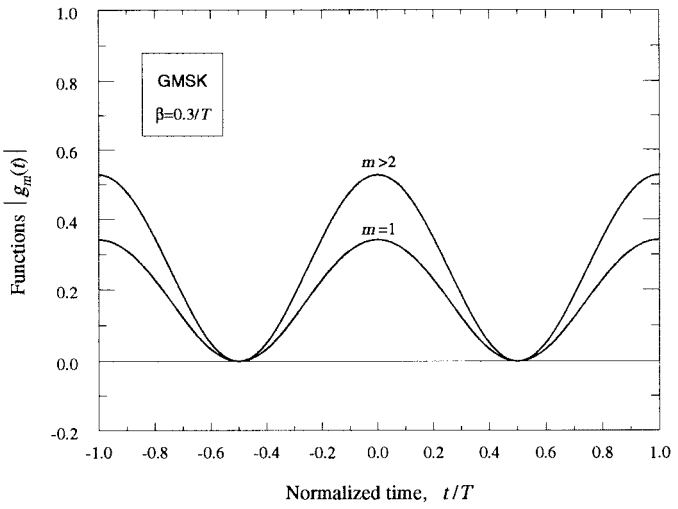

Fig. 1. Shape of $|g_m(t)|$ for GMSK.

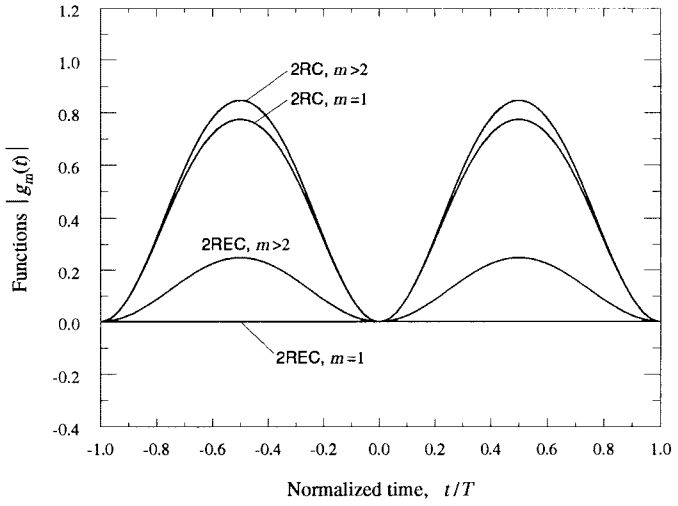

Fig. 2. Shape of $|g_m(t)|$ for 2REC and 2RC.

A. Timing Estimation

To proceed, we eliminate ν in (14) by taking the amplitudes of both sides. Assuming for simplicity that the noise term is negligible, we get

$$|R_m(t)| = |g_m(t-\tau)|. \tag{19}$$

It is readily seen from (16) that $g_m(t)$ is a periodic function of time and, as such, it can be expanded into a Fourier series. Also, in the Appendix it is shown that $g_m(t)$ is even and, therefore, the series takes the simple form

$$|g_m(t)| = A_0(m) + 2\sum_{k=1}^{\infty} A_k(m)\cos\left(\frac{2\pi kt}{T}\right) \tag{20}$$

where $A_k(m)$ are real coefficients

$$A_k(m) = \frac{1}{T}\int_0^T |g_m(t)|\cos(2\pi kt/T)\,dt \quad k = 0, 1, \cdots. \tag{21}$$

Figs. 1 and 2 illustrate the shape of $|g_m(t)|$ for GMSK, 2RC, and 2REC modulation. It is seen that, in general, $|g_m(t)|$ looks like a raised cosine function of period T. One singular case occurs with the 2REC format and $m = 1$, wherein $|g_1(t)|$ is identically zero. These facts indicate that the first two terms in the sum (20) dominate the series and, therefore, $|g_m(t)|$ can be accurately approximated as

$$|g_m(t)| \approx A_0(m) + 2A_1(m)\cos\left(\frac{2\pi t}{T}\right). \tag{22}$$

Correspondingly, (19) becomes

$$|R_m(t)| \approx A_0(m) + 2A_1(m)\cos\left[\frac{2\pi(t-\tau)}{T}\right]. \tag{23}$$

It should be noted that (23) is an exact result for MSK. In fact, the absolute value of (18) is seen to coincide with (22) for $A_0(m) = 1/2$ and $A_1(m) = 1/4$.

Now, suppose that the autocorrelations $\{R_m(t)\}$, $1 \le m \le M$ are available. How can we exploit them to estimate the timing epoch? We propose a method based on a linear combination of the magnitudes $|R_m(t)|$. In particular, we consider the following function:

$$\xi(t) = \sum_{m=1}^{M} A_1(m)|R_m(t)|. \tag{24}$$

As is now explained, the location of the maximum of $\xi(t)$ gives an estimate of τ. To see why this is so, let us substitute (23) into (24). As a result, we get

$$\xi(t) = B_0 + 2B_1\cos\left[\frac{2\pi(t-\tau)}{T}\right] \tag{25}$$

with

$$B_n = \sum_{m=1}^{M} A_1(m)A_n(m) \quad n = 0, 1. \tag{26}$$

Since $B_1 > 0$, it is clear from (25) that $\xi(t)$ is maximum at $t = \tau$. It should be recalled, however, that (25) holds true only for negligible noise levels. In general, the noise will not be negligible and the peak of $\xi(t)$ will give only an estimate of τ.

Based on the above results, we now compute the location of the peak of $\xi(t)$. To this end, let us denote by $\xi(i)$ and $R_m(i)$ the samples of $\xi(t)$ and $R_m(t)$ taken at the times $t = iT/N$. Then, from (25) we have

$$\xi(i) = B_0 + B_1 e^{-j2\pi\tau/T}e^{j2\pi i/N} + B_1 e^{j2\pi\tau/T}e^{-j2\pi i/N}. \tag{27}$$

Taking the Fourier transform and rearranging yields (for $N \ge 3$)

$$\tau = -\frac{T}{2\pi}\arg\left\{\sum_{i=0}^{N-1}\xi(i)e^{-j2\pi i/N}\right\} \tag{28}$$

which says that, if the autocorrelation samples $R_m(i)$ were available, $\xi(i)$ could be computed from (24) as

$$\xi(i) = \sum_{m=1}^{M} A_1(m)|R_m(i)| \tag{29}$$

and then, substituting into (28), we would get the desired estimate. The estimate would be exact in the absence of noise.

Unfortunately, the samples $R_m(i)$ are not available and must be estimated from the data $x_k(i)$. A simple method to do so is to replace the $R_m(i)$ by the *sample autocorrelations*

$$\hat{R}_m(i) = \frac{1}{L_0 - m} \sum_{k=m}^{L_0-1} \left[x_k(i) x_{k-m}^*(i)\right]^2, \quad 0 \le i \le N-1, \quad 1 \le m \le M. \tag{30}$$

Thus, an estimate $\hat{\tau}$ of τ can be derived from (28) by replacing $\xi(i)$ by

$$\hat{\xi}(i) = \sum_{m=1}^{M} A_1(m) \left|\hat{R}_m(i)\right|, \qquad 0 \le i \le N-1. \tag{31}$$

In other words, we have

$$\hat{\tau} = -\frac{T}{2\pi} \arg \left\{ \sum_{i=0}^{N-1} \left[\sum_{m=1}^{M} A_1(m) \left|\hat{R}_m(i)\right| \right] e^{-j2\pi i/N} \right\}. \tag{32}$$

B. Frequency Offset Estimation

Returning to the autocorrelation in (14), we see that its useful component has a time-varying amplitude, $|g_m(t-\tau)|$. As we want to use $R_m(t)$ for estimating ν, we think it beneficial to exploit the sample of $R_m(t)$ at the instant $\bar{t}_m$ where $|g_m(t-\tau)|$ is maximum. From (22) we have

$$\bar{t}_m = \tau + \eta_m T \tag{33}$$

with η_m given by

$$\eta_m = \begin{cases} 0, & \text{if } A_1(m) > 0 \\ 1/2, & \text{otherwise.} \end{cases} \tag{34}$$

To go further, we now consider the quantities

$$\rho_m = R_m(\bar{t}_m) R_{m-1}^*(\bar{t}_{m-1}), \qquad 1 \le m \le M \tag{35}$$

in which $R_0(\bar{t}_0)$ is arbitrarily defined equal to unity. Substituting (14) into (35) and neglecting the noise for simplicity yields

$$\rho_m = e^{j4\pi\nu T} g_m(\eta_m T) g_{m-1}(\eta_{m-1} T). \tag{36}$$

Next, let us define

$$\mu_m = \begin{cases} 1, & \text{if } g_m(\eta_m T) g_{m-1}(\eta_{m-1} T) > 0 \\ -1, & \text{otherwise.} \end{cases} \tag{37}$$

Multiplying (36) by μ_m, taking the arguments of both sides, summing for m over $1 \le m \le M$ and, finally, using (35) produces

$$\nu = \frac{1}{4\pi MT} \sum_{m=1}^{M} \arg\left\{\mu_m R_m(\bar{t}_m) R_{m-1}^*(\bar{t}_{m-1})\right\}. \tag{38}$$

This relation indicates a method to compute ν from the samples $\{R_m(\bar{t}_m)\}$. It should be noted that the coefficients $\{\mu_m\}$ are uniquely specified by the modulation format [see (37) and (16)] and, therefore, they can be precomputed.

It remains to be seen how to get the samples $R_m(\bar{t}_m)$. One obvious approach is to approximate them with the sample autocorrelations $\{\hat{R}_m(i)\}$ we have already exploited for the estimation of τ. Recalling that $\hat{R}_m(i)$ is an estimate of $R_m(iT/N)$, it would seem natural to replace $R_m(\bar{t}_m)$ by that particular $\hat{R}_m(i)$, say $\hat{R}_m(i_m)$, such that $i_m T/N$ is closest to $\bar{t}_m$. Unfortunately, from (33) it is clear that the exact value of $\bar{t}_m$ is unknown (since so is τ). Then, as a second choice we take that $i_m T/N$ which is closest to $\hat{\tau} + \eta_m T$, where $\hat{\tau}$ is given in (32). In formulas, we have

$$i_m = \underset{0 \le i \le N-1}{\arg\min} \left\{ \left| \left[\hat{\tau} + \eta_m T - i\frac{T}{N} \right]_{-T/2}^{T/2} \right| \right\} \tag{39}$$

where $[x]_{-T/2}^{T/2}$ means the value of x reduced to the interval $[-T/2, T/2)$. In conclusion, the frequency offset estimate is expressed by

$$\hat{\nu} = \frac{1}{4\pi MT} \sum_{m=1}^{M} \arg\left\{\mu_m \hat{R}_m(i_m) \hat{R}_{m-1}^*(i_{m-1})\right\}. \tag{40}$$

C. Summary and Comments

The estimation procedure described above develops through the following steps:

1) compute the MN autocorrelations $\{\hat{R}_m(i)\}$ from (30);
2) estimate the timing epoch from (32);
3) compute the N indexes i_m from (39) and select the M autocorrelations $\hat{R}_m(i_m)$;
4) estimate $\hat{\nu}$ from (40).

It is worth stressing that coefficients $A_1(m)$, η_m, and μ_m appearing in (32), (39), and (40) depend only on the modulation format and can be precomputed.

The following remarks about the proposed algorithm are of interest.

1) For MSK modulation, it turns out that $A_1(m) = 1/4$, $\eta_m = 0$, and $\mu_m = -1$ for any m. Correspondingly, the timing and frequency estimates become

$$\hat{\tau} = -\frac{T}{2\pi} \arg\left\{ \sum_{i=0}^{N-1} \left[\sum_{m=1}^{M} |\hat{R}_m(i)| \right] e^{-j2\pi i/N} \right\} \tag{41}$$

$$\hat{\nu} = \frac{1}{4\pi MT} \sum_{m=1}^{M} \arg\left\{-\hat{R}_m(i_m) \hat{R}_{m-1}^*(i_{m-1})\right\}. \tag{42}$$

   In particular, for $M = 1$, these estimates coincide with those proposed by Mehlan, Chen, and Meyr (MCM) in [11]. Thus, our method may be viewed as an extension of the MCM algorithm in two directions. On one side, as it employs autocorrelations with indexes $m > 1$ (in addition to those with $m = 1$), it better exploits the available data. On the other side, it can be used with any MSK-type format, not just MSK. As we shall see shortly, the application of the MCM method to narrow-band modulations such as GMSK gives poor results.

2) Computing the timing and frequency estimates as indicated in (32) and (40) requires approximately $NM(4L_0 - 2M + 5) + N(3L_0 + 4)$ real products and $NM(4L_0 - 2M + 2) + N(L_0 + 1)$ real additions. These figures take into account the fact that: a) a complex multiplication is equivalent to four (real) multiplications

and two (real) additions; b) a modulus extraction requires two multiplications and one addition; c) squaring a complex number requires three multiplications and one addition. It is seen that the complexity of the proposed algorithm increases as M grows large and is about M times larger than the MCM method (MN autocorrelations need to be computed instead of just N). Whether this extra complexity is justified depends to a large extent on the modulation format. Simulations indicate that M-values greater than unity are necessary for narrow-band formats.

3) So far we have concentrated on the estimates $\hat{\tau}(0)$ and $\hat{\nu}(0)$ obtained from the first subsequence $\{x_k(i)\}_{(0)}$. As the others can be computed in a similar manner, the question arises of how to put all these results together. We begin with the timing estimates. To understand the problem, take note that the sampling rate is a multiple of the *nominal* symbol rate, not the *actual* symbol rate (which is unknown at the receiver). As a consequence, the sampling times will slowly drift relative to the symbol times and the parameter τ will not remain constant, as we assumed earlier. In fact, we expect that $\hat{\tau}(l)$ will change from one subsequence to the other. Furthermore, as the estimates $\hat{\tau}(l)$ are limited to the interval $\pm T/2$, they will occasionally make jumps of $\pm T$ in passing from one subsequence to the other. This is a manifestation of the so-called *unwrapping problem*. Clearly, the jumps must be properly compensated to avoid synchronization errors. A simple way to do so is indicated in [12] and consists of processing the $\hat{\tau}(l)$ according to the formula

$$\hat{\hat{\tau}}(l+1) = \hat{\hat{\tau}}(l) + \text{saw}_T[\hat{\tau}(l+1) - \hat{\hat{\tau}}(l)], \quad l = 0, 1, 2, \cdots \tag{43}$$

where $\text{saw}_T(x)$ is a saw-tooth nonlinearity that reduces x to the interval $\pm T/2$. It is easily checked that the compensated sequence $\hat{\hat{\tau}}(l)$ has no breaches of continuity.

As for the frequency estimates, in the next section we show that the maximum allowed frequency offset is greater than 10% of the symbol rate, which is sufficient for most practical applications. Under these circumstances, the frequency estimates need not be unwrapped and we can put $\hat{\hat{\nu}}(l) = \hat{\nu}(l)$.

IV. Simulation Results

In this section we report on simulation results illustrating the performance of the proposed synchronizer on AWGN and Rayleigh fading channels. We begin with a short description of the simulation model. The receiver filter bandwidth must be large enough not to distort the signal components (even in the presence of the allowed frequency offsets) but not too large to pass unnecessary noise. As a break-even point, we have chosen an eight-pole Butterworth finite impulse response (FIR) filter with a 3-dB bandwidth $B_w = 0.75/T$. This allows us to handle frequency offsets up to 15% of the bit rate. The oversampling factor N has been set to four, and the observation length L_0 to 128 (unless otherwise specified). With GMSK modulation, a premodulator bandwidth $B = 0.3/T$ has been chosen.

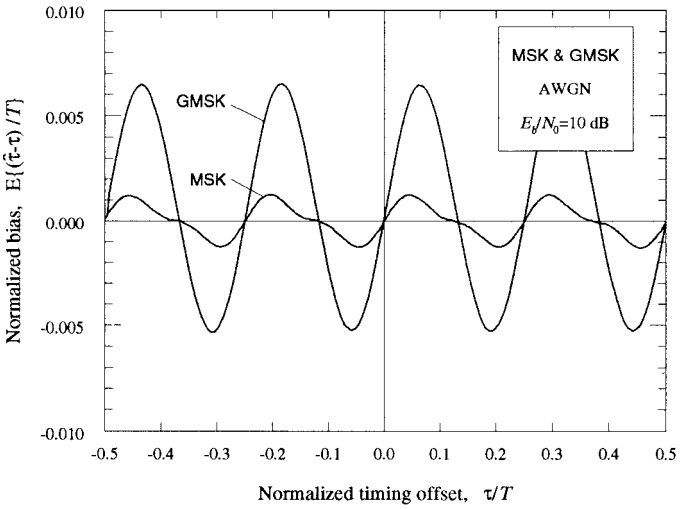

Fig. 3. Bias of the timing estimates for GMSK and MSK with $M = 4$ and AWGN.

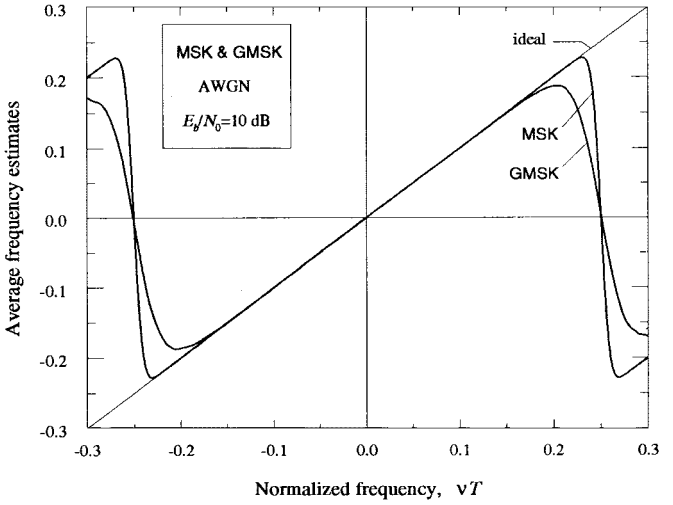

Fig. 4. Average frequency estimates for GMSK and MSK with $M = 4$ and AWGN.

A. AWGN Channel

Fig. 3 illustrates the normalized bias of the timing estimates (32) as a function of τ/T. The signal-to-noise ratio is 10 dB and the frequency offset is zero. The parameter M is chosen equal to four. It is seen that the bias has a periodic pattern of period $T/4$. Its peaks are about 10^{-3} for MSK and $6 \cdot 10^{-3}$ for GMSK and are quite tolerable for most applications.

Fig. 4 shows the average frequency estimates $E\{\hat{\nu}T\}$ as a function of νT, for $E_b/N_0 = 10$ dB and $M = 4$. The timing parameter τ is set to zero, but similar results are obtained for other timing epochs. The ideal line $E\{\hat{\nu}T\} = \nu T$ is also drawn as a reference. It appears that the estimates are unbiased over the range $|\nu T| < 0.15$ for GMSK and $|\nu T| < 0.2$ for MSK. These conclusions do not change with M-values other than four. It turns out, however, that the estimation range depends somewhat on the SNR and gets narrower as E_b/N_0 decreases.

To make a practical example, consider the GSM mobile cellular system (with a carrier frequency of 900 MHz and a symbol rate of 270 kbit/s). With an estimation range $|\nu T| <$

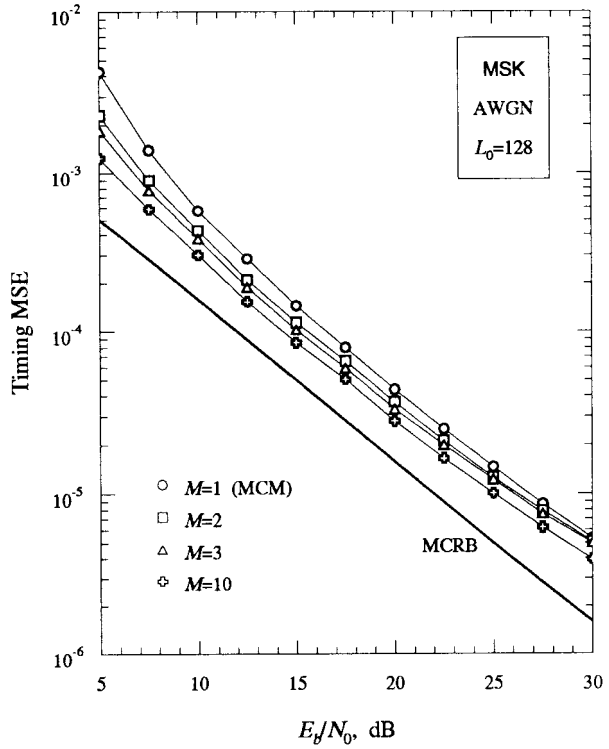

Fig. 5. Timing MSE for MSK and AWGN.

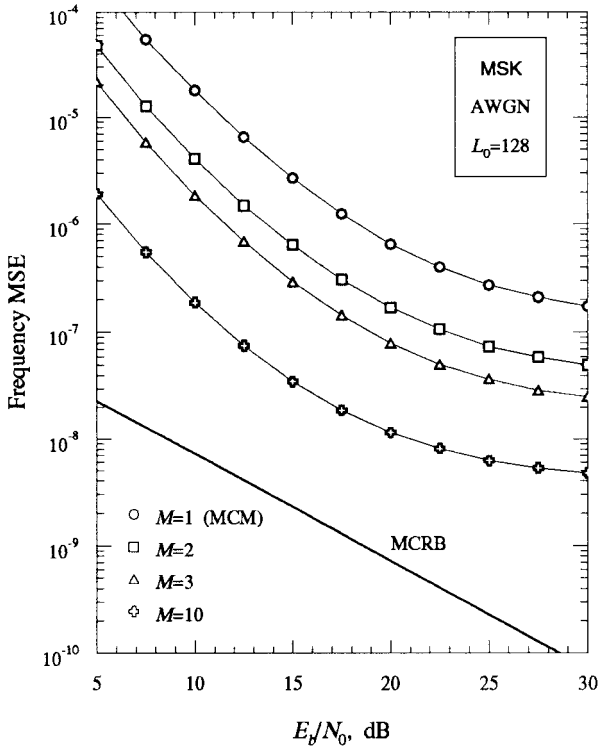

Fig. 6. Frequency MSE for MSK and AWGN.

0.15, the maximum allowed difference between transmitter and receiver frequencies is about 40 kHz. Assuming that 20 kHz may be ascribed to the instability of the transmitter oscillator and the remainder to that of the receiver oscillator, it follows that the oscillator's accuracy must be better than ± 22 ppm. This goal is easily achieved since ordinary synthesizers have stabilities on the order of ± 5 ppm.

Figs. 5 and 6 illustrate the normalized timing and frequency mean square errors (MSEs), $E\{[(\hat{\tau}-\tau)/T]^2\}$, and $E\{[(\hat{\nu}-\nu)T]^2\}$ as a function of E_b/N_0 for MSK. Marks indicate simulation results while solid lines are drawn to ease the reading. The modified Cramer–Rao bounds (MCRBs) for timing and frequency estimation are also shown as benchmarks. They are expressed by [13, p. 61 and 68]

$$\mathrm{MCRB}(\tau) = \frac{T(E_b/N_0)^{-1}}{2\pi^2 \xi L_0} \tag{44}$$

$$\mathrm{MCRB}(\nu) = \frac{3(E_b/N_0)^{-1}}{2\pi^2 T^2 L_0^3} \tag{45}$$

with

$$\xi = \int_0^{LT} h^2(t)\,dt. \tag{46}$$

All the results have been obtained by modeling τ and ν as random variables uniformly distributed over the intervals $(-T/2, T/2)$ and $(-0.15/T, 0.15/T)$. It is seen that the estimation accuracy improves as M increases. Actually, the improvement is rather limited with timing estimation, whereas it is substantial with frequency estimation. For example, the MSE with $M = 3$ is about one order of magnitude smaller than with $M = 1$.

Simulations related to GMSK are shown in Figs. 7 and 8. As anticipated, the performance with $M = 1$ is poor both with timing and frequency estimation. It is seen, however, that dramatic improvements are obtained with M-values as small as 2–3. This confirms the claim that the proposed estimation scheme is applicable even with narrow-band modulation. Other simulations obtained with other modulation formats (but not shown for space limitations) are in keeping with this conclusion.

B. Flat-Fading Channel

In a Rayleigh flat-fading channel, the received signal is affected by a multiplicative distortion (MD) which can be modeled as a zero-mean complex Gaussian process. In the simulations to follow, the real and imaginary components of MD have been generated by filtering two independent real Gaussian processes in two identical third-order Butterworth filters. The 3-dB bandwidth B_D of these filters is taken as a measure of the fading rate.

Figs. 9 and 10 illustrate the timing and frequency MSE versus $\bar{E}_b/N_0$ for GMSK ($\bar{E}_b$ denotes the average received signal energy per symbol). Comparing with Figs. 7 and 8 indicates that the synchronizer performance is significantly degraded with respect to the AWGN channel. Also, the degradation increases as the fading rate grows larger.

C. Frequency-Selective Fading Channel

In digital transmission over frequency selective fading channels, it is common practice to use fractionally spaced equalizers which are rather insensitive to timing errors. Accordingly, in the ensuing discussion we limit ourselves to frequency esti-

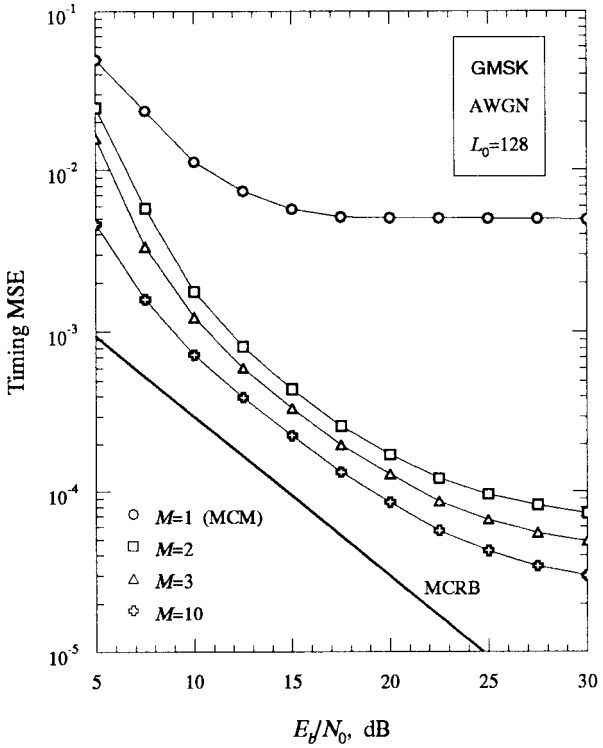

Fig. 7. Timing MSE for GMSK and AWGN.

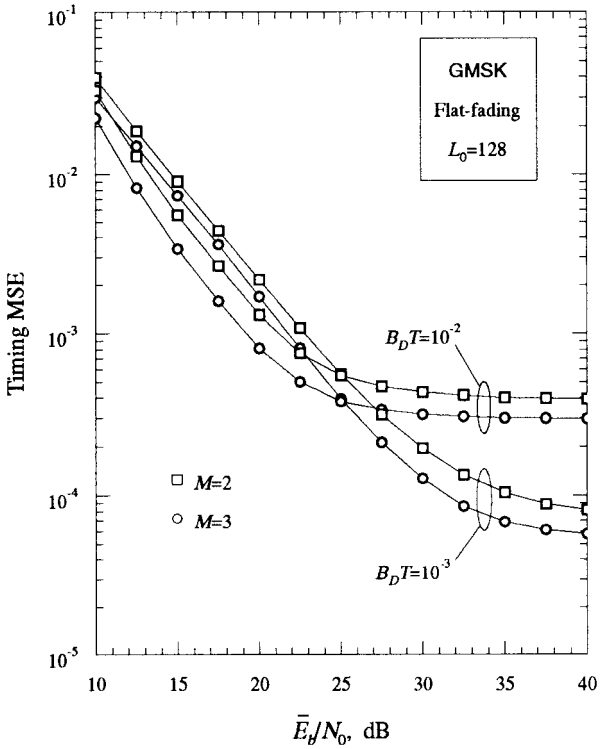

Fig. 9. Timing MSE for GMSK and Rayleigh flat-fading.

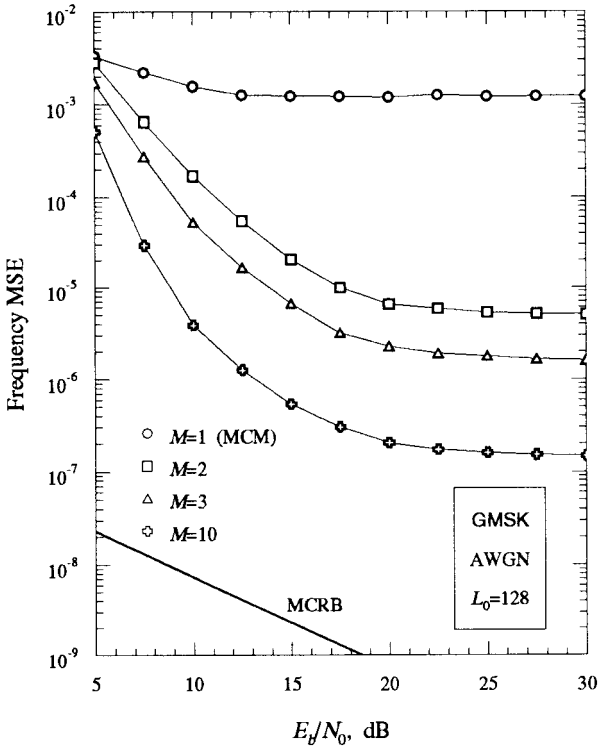

Fig. 8. Frequency MSE for GMSK and AWGN.

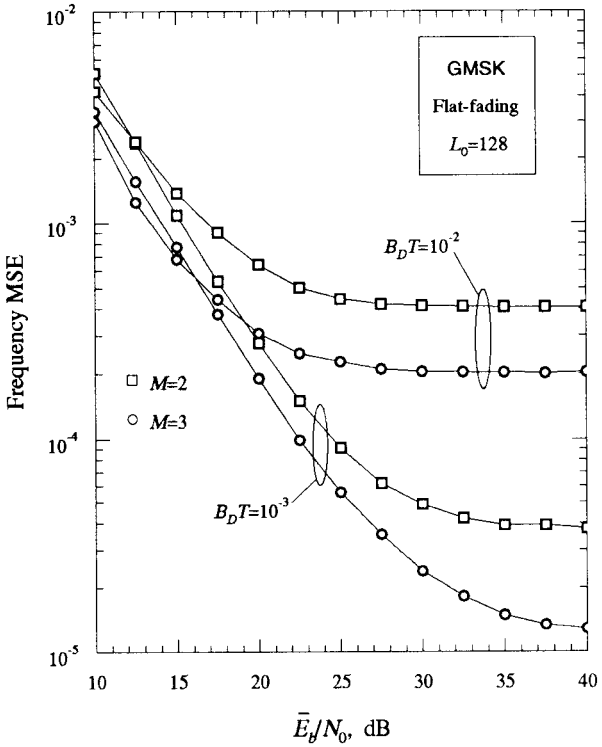

Fig. 10. Frequency MSE for GMSK and Rayleigh flat-fading.

mation only. The propagation delays and attenuation factors of the multipath channel are taken from the typical urban power delay profile of the GSM channel model [14]. In particular, the propagation delays are fixed, whereas the attenuation factors are generated by passing independent zero-mean complex Gaussian processes through a third-order Butterworth filter with a 3-dB bandwidth $B_D = 10^{-2}/T$.

Simulations obtained with narrowband modulations indicate that, even at relatively high $\bar{E}_b/N_0$ values, the frequency estimates are occasionally affected by large errors (outliers).

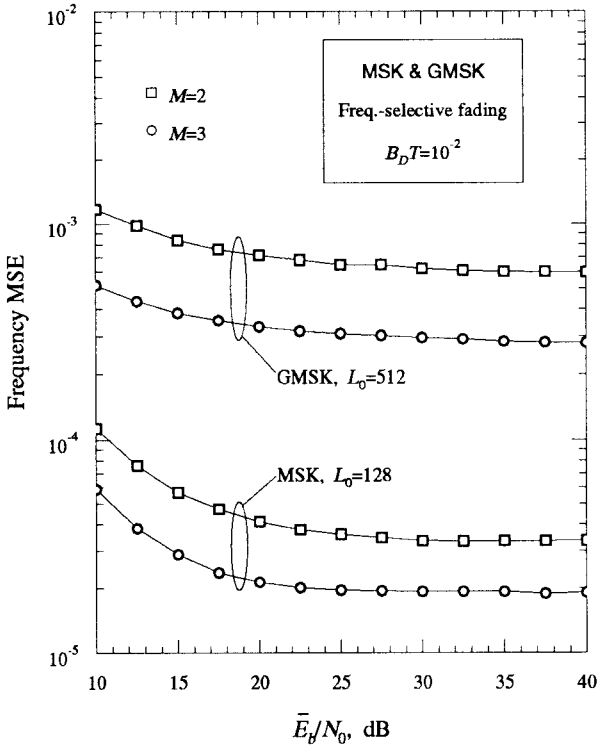

Fig. 11. Frequency MSE with Rayleigh frequency selective fading.

A way to alleviate this problem is to increase the estimation interval. Fig. 11 illustrates the frequency MSE versus $\bar{E}_b/N_0$ for MSK and GMSK. Comparing with Fig. 10 indicates that the performance with GMSK and frequency selective fading can be made close to that obtained with flat fading by using an observation length four times longer. On the other hand, satisfactory performance for MSK over frequency-selective fading is obtained even with $L_0 = 128$. Further simulations (not shown for space limitations) indicate that the frequency estimates are unbiased over the range $|\nu T| < 0.15$ for GMSK and $|\nu T| < 0.2$ for MSK (as happens with AWGN).

V. Conclusion

A new nondata-aided synchronization method has been proposed for joint frequency and timing estimation with MSK-type signaling. The synchronizer has a feedforward structure that is suitable for digital implementation. Frequency offsets up to 15% of the bit rate can be estimated. The algorithm may be viewed as a generalization of the method studied in [11] for MSK. Compared with the latter, it has a larger applicability and, in fact, it can be used even with narrow-band modulations like GMSK. Its complexity is proportional to an integer parameter M. For $M = 1$, the algorithm has the same complexity as that in [11] and approximately requires $28(L_0 + 1)$ multiplications and $20L_0 + 4$ additions if an oversampling factor $N = 4$ is chosen. Simulations indicate that, in many cases, $M = 2$ is sufficient to achieve good performance with either AWGN or Rayleigh fading channels. Under these circumstances, only $48L_0+24$ multiplications and $36L_0 - 12$ additions are required.

Appendix

In this Appendix we compute the expectation in (15) of the text. To proceed, collecting (2) and (15) yields

$$g_m(t) = E\left\{ \prod_{n=-\infty}^{+\infty} e^{j2\pi\alpha_n p_m(t-nT)} \right\} \tag{A1}$$

where

$$p_m(t) = q(t) - q(t - mT). \tag{A2}$$

Next, assuming that the transmitted symbols are statistically independent and equiprobable, the expectation in (A1) can be carried out in a factor-by-factor fashion to produce

$$g_m(t) = \prod_{n=-\infty}^{+\infty} E\{e^{j2\pi\alpha_n p_m(t-nT)}\} \tag{A3}$$

or, equivalently,

$$g_m(t) = \prod_{n=-\infty}^{+\infty} \{\cos[2\pi p_m(t - nT)] + jE\{\alpha_n\}\sin[2\pi p_m(t - nT)]\}. \tag{A4}$$

On the other hand, since $E\{\alpha_n\} = 0$, (A4) reduces to

$$g_m(t) = \prod_{n=-\infty}^{+\infty} \cos[2\pi p_m(t - nT)]. \tag{A5}$$

At this point it is useful to recall that the phase pulse $q(t)$ satisfies the relation (9) in the text. Thus, collecting such a relation with (A2) produces

$$p_m(-t) = p_m(t + mT + LT). \tag{A6}$$

Then, from (A5) and (A6) we get

$$g_m(-t) = \prod_{n=-\infty}^{+\infty} \cos[2\pi p_m(t + nT + mT + LT)] \tag{A7}$$

and comparing with (A5) we see that $g_m(t) = g_m(-t)$, which says that $g_m(t)$ is even.

Acknowledgment

The authors would like to thank the anonymous reviewers for their helpful comments which have improved the quality of the paper.

References

[1] J. B. Anderson, T. Aulin, C.-E. Sundberg, *Digital Phase Modulation.* New York: Plenum, 1986.
[2] P. Galko and S. Pasupathy, "On a class of generalized MSK," in *Proc. Int. Conf. Communications*, Denver, CO, June 1981, pp. 2.4.1–2.4.5.
[3] T. Masamura, S. Shuichi, M. Morihiro, and H. Fuketa, "Differential detection of MSK with nonredundant error correction," *IEEE Trans. Commun.*, vol. COM-27, pp. 912–920, June 1979.
[4] G. Kaleh, "A differentially coherent receiver for minimum shift keying signal," *IEEE J. Select. Areas Commun.*, vol. 7, pp. 99–106, Jan. 1989.
[5] D. Makrakis, A. Yongacoglu, and K. Feher, "Novel receiver structures for systems using differential detection," *IEEE Trans. Veh. Technol.*, vol. VT-36, pp. 71–77, May 1987.
[6] M. K. Simon and C. C. Wang, "Differential detection of Gaussian MSK in a Mobile radio environment," *IEEE Trans. Veh. Technol.*, vol. VT-33, pp. 307–319, Nov. 1984.

[7] R. de Buda, "Coherent demodulation of frequency-shift keying with low deviation ratio," *IEEE Trans. Commun.*, vol. COM-20, pp. 429–435, June 1972.
[8] A. N. D'Andrea, U. Mengali, and R. Reggiannini, "A digital approach to clock recovery in generalized minimum shift keying," *IEEE Trans. Veh. Technol.*, vol. 39, pp. 227–234, Aug. 1990.
[9] M. Luise and R. Reggiannini, "An efficient carrier frequency recovery scheme for GSM receivers," in *GLOBECOM'92, Conf. Rec. Communications Theory Mini-Conf.*, Orlando, FL, Dec. 6–9, pp. 36–40.
[10] A. N. D'Andrea, A. Ginesi, and U. Mengali, "Frequency detectors for CPM signals," *IEEE Trans. Commun.*, vol. 43, pp. 1828–1837, Apr. 1995.
[11] R. Mehlan, Y.-E. Chen, and H. Meyr, "A fully digital feedforward MSK demodulator with joint frequency offset and symbol timing estimation for burst mode mobile radio," *IEEE Trans. Veh. Technol.*, vol. 42, pp. 434–443, Nov. 1993.
[12] M. Oerder and H. Meyr, "Digital filter and square timing recovery," *IEEE Trans. Commun.*, vol. COM-36, pp. 605–611, May 1988.
[13] U. Mengali and A. N. D'Andrea, *Synchronization Techniques for Digital Modems.* New York: Plenum, 1997.
[14] GSM Recommendation 05.05, *Radio Transmission and Reception*, ETSI/PT 12, V. 3.11.0, Jan. 1990.

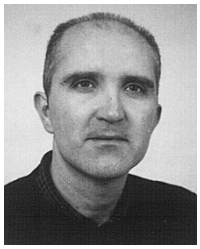

Michele Morelli was born in Pisa, Italy, in 1965. He received the Laurea (cum laude) in electronic engineering and the "Premio di Laurea SIP" from the University of Pisa, Italy, in 1991 and 1992 respectively. From 1992 to 1995 he was with the Department of Information Engineering at the University of Pisa, where he received the Ph.D. degree in electrical engineering.

He is currently a Research Fellow at the Centro Studi Metodi e Dispositivi Radiotrasmissioni of the Italian National Research Council (CNR) in Pisa. His interests are in digital communication theory, with emphasis on synchronization algorithms.

Umberto Mengali (M'69–SM'85–F'90) received his education in electrical engineering from the University of Pisa. In 1971 he obtained the Libera Docenza in telecommunications from the Italian Education Ministry.

Since 1963 he has been with the Department of Information Engineering, University of Pisa, Pisa, Italy, where he is a Professor of Telecommunications. In 1994 he was a Visiting Professor at the University of Canterbury, New Zealand, as an Erskine Fellow. His research interests are in digital communications and communication theory, with emphasis on synchronization methods and modulation techniques. He has published approximately 80 journal papers and has co-authored *Synchronization Techniques for Digital Receivers* (Plenum, 1997).

Prof. Mengali is a member of the Communication Theory Committee and has been an Editor of the IEEE TRANSACTIONS ON COMMUNICATIONS from 1985 to 1991. He is now Editor for Communication Theory of the *European Transactions on Telecommunications*. He is listed in *American Men and Women in Science*.